Internal Electric Field at the Schottky Junctions in MXene-MnCdS Heterostructure for Complete Uranium Remediation

Luowen Xv, Yan Liu*, Changfu Wang, Zhirong Liu, Yun Tian, Fengtao Yu, Yun Wang, Dingzhong Yuan, Hao Jiang*

National Key Laboratory of Uranium Resources Exploration-Mining and Nuclear Remote Sensing, East China University of Technology, Nanchang, Jiangxi 330013, PR China.

* Corresponding author: E-mail: fzliuyan1986@163.com; jianghao@ecut.edu.cn

Chemicals and materials

Titanium aluminium carbide (Ti_3AlC_2, ≥99.9%), cadmium acetate dihydrate ($Cd(CH_3COO)_2 \cdot 2H_2O$, AR), manganese acetate tetrahydrate ($Mn(CH_3COO)_2 \cdot 4H_2O$, 99.99%), uranyl nitrate hexahydrate ($UO_2(NO_3)_2 \cdot 6H_2O$, AR), and thiourea (CH_4N_2S, ≥99%) were acquired from Aladdin Biochemical Technology Company. None of the reagents employed is in need of purification.

Synthesis of $Ti_3C_2T_x$

2 g of LiF was added to 40 mL of 9 M hydrochloric acid in a Teflon container, followed by stirring in a 40 °C oil bath (600 rpm) for 30 min to dissolve LiF. Subsequently, 2 g of Ti_3AlC_2 powder was gradually added to the solution, and etching was conducted at 40 °C for 48 h with continuous stirring. The resulting black suspension was centrifuged (5000 rpm, 10 min) with 2 M HCl to remove unreacted LiF and Al^{3+} impurities, then washed repeatedly with deionized water until the supernatant pH reached 6.0. The suspension was ultrasonicated in an ice bath for 1.5 h and centrifuged (3500 rpm, 20 min) to obtain a monolayer $Ti_3C_2T_x$ suspension, which was vacuum-dried at 60 °C for 12 h to yield $Ti_3C_2T_x$ powder.

Synthesis of $Mn_xCd_{1-x}S@Ti_3C_2T_x$

A mixture comprising 3 mmol of $Mn(CH_3COO)_2 \cdot 4H_2O$, 7 mmol of $Cd(CH_3COO)_2 \cdot 2H_2O$ and 10 mmol of CH_4N_2S was dissolved in 40 mL of deionized water and stirred for 1 h. Subsequently, a specific amount of $Ti_3C_2T_x$ suspension was introduced into the stirred solution and transferred to the reaction kettle maintained at 160 °C for 24 h. Finally, the resultant materials were washed three times with deionized water and ethanol prior to overnight drying under vacuum, resulting in the formation of $Mn_xCd_{1-x}S@Ti_3C_2T_x$ composite.

Adsorption experiment

The adsorption isotherm is carried out by adding 10 mg composites to the 50 mL uranium solution of 0-200 ppm. After a specific time, the supernatant is fetched through 0.22 μm syringe filter, whereas the uranium concentration is determined using the arsenazo III method with an ultraviolet-visible spectrophotometer.

The adsorption capacity and removal efficiency of Uranium is calculated as:

$$q_e = \frac{(C_0 - Ce) \times V}{m} \qquad (1)$$

$$R(\%) = \frac{(C_0 - Ce) \times 100\%}{C_0} \qquad (2)$$

where V is the volume of the treated solution (L), m is the amount of used adsorbent, and C_0 and C_e are the initial concentration and the final equilibrium concentration of uranium, respectively.

Photocatalysis experiment

The photocatalytic experiments were conducted by introducing 10 mg of the photocatalyst into 50 mL of a 100 ppm uranium solution, without the addition of any sacrificial agent. Prior to illumination, adsorption-desorption equilibrium was established by stirring at room temperature in darkness for 30 min. This was followed by irradiating the solution under a 300 W xenon lamp for 30 min, with samples being collected every 5 min. The concentration of uranium was determined by UV-visible spectrophotometer using the arsenazo (III) method.

Theoretical calculation

First-principles calculations were performed within the theoretical framework of DFT, utilizing the projector augmented plane-wave method implemented in the Vienna Ab Initio Simulation Package (VASP).

Characterization

The morphology and microstructure of the photocatalysts were characterized using Transmission Electron Microscopy (TEM, FEI Talos F200S) and Scanning Electron Microscopy (SEM, Sigma300). Elemental analysis was conducted employing Energy Dispersive X-ray Spectroscopy (EDS). The surface morphology and electrical properties of the materials were characterized by Atomic Force Microscope and Kelvin Probe Force microscopy (AFM and KPFM, Bruker Dimension Icon). Fourier Transform Infrared spectroscopy (FT-IR, Thermo Fisher Scientific Nicolet iS5) was utilized to analyze the composition of functional groups in the samples. The crystal structure of the sample was examined by X-ray Powder Diffraction (XRD, Bruker D8 Advance) while X-ray photoelectron spectroscopy (XPS, Thermo Scientific Nexsa) was employed for studying the composition and valence of the elements. Brunauer-Emmett-Teller (BET, V-Sorb 2800TP) was used for specific surface area analysis. The visible diffuse reflectance spectrum of UV-vis was measured with a UV-vis light spectrophotometer (UV-vis DRS Shimadzu UV-3600i Plus). Active substances during the reaction were determined by Electron Paramagnetic Resonance spectroscopy (EPR, Bruker ESR5000). The Photoluminescence spectrum (PL) analyzed was performed utilizing a fluorescence spectrophotometer (Edinburgh FLS1000). Transient photocurrent and Electrochemical Impedance Spectroscopy (EIS) measurements in a standard three-electrode system were carried out on a CHI 660E electrochemical workstation with platinum as the working electrode and Ag/AgCl as the reference electrode. The surface charge properties of the materials under different pH conditions were analyzed using a Zeta potential analyzer (Malvern Zetasizer Nano ZS). Charge separation efficiency and carrier migration kinetics were investigated by transient photovoltage (TPV) measurements performed on a CEL-SPS1000 test system.

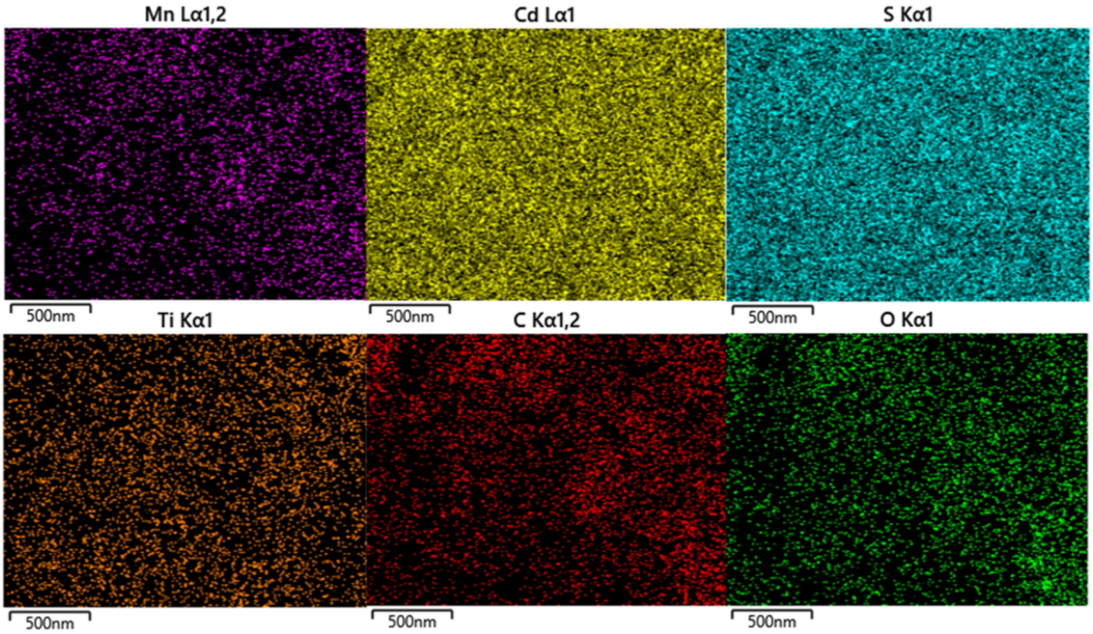

Fig. S1 The SEM-EDS element mapping images of MCS@TC-15.

Table S1 BET results of $Mn_{0.3}Cd_{0.7}S$, $Ti_3C_2T_x$ and MCS@TC-15.

Sample	BET Surface Area (m^2/g)	Pore Volume (cm^3/g)	Pore Size (nm)
$Mn_{0.3}Cd_{0.7}S$	86.36	0.45	13.55
$Ti_3C_2T_x$	93.21	0.70	19.10
MCS@TC-15	104.99	0.28	7.86

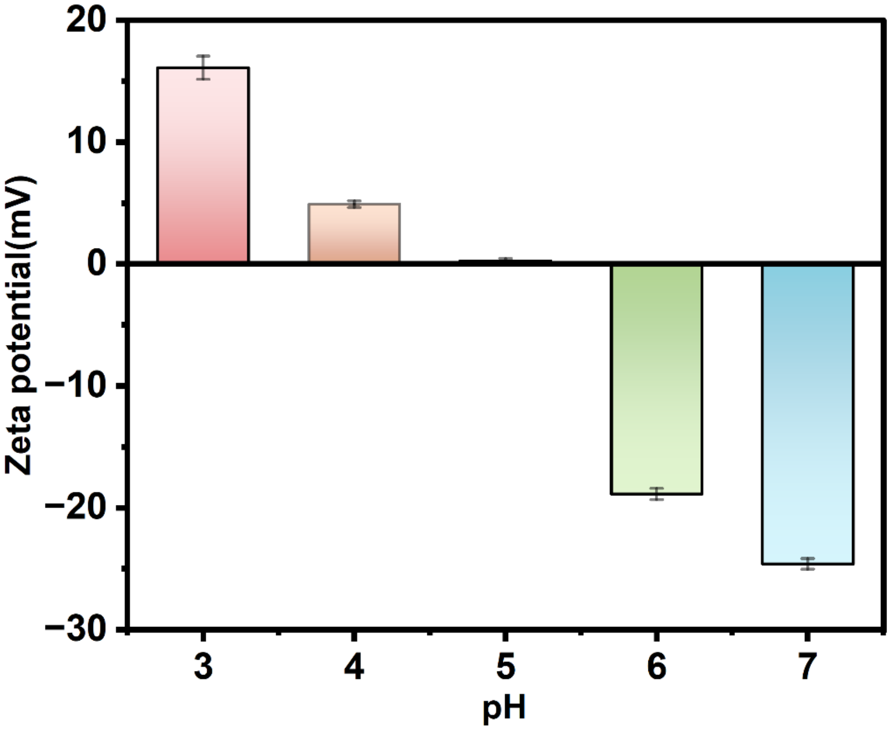

Fig. S2 Zeta potential of MCS@TC-15 at different pH values.

Table S2 Comparison of photocatalytic properties for U(VI) by different photocatalysts.

Photocatalysts	**Light source**	**Photocatalytic conditions**	**Electron sacrifice**	**Reaction time**	**Removal efficiency (%)**	**Ref.**
NC-GCN/Ag_2O	300 W Xe lamp	C_0=20 mg/L, pH=5, V=50 mL, m=10 mg	CH_3OH	30min	93.2	4
g-C_3N_4@attapulgite	LED lamp	C_0=20 mg/L, pH=6, V=100 mL, m=0.1 mg	CH_3OH	70 min	98.4	5
OPFCN	300 W Xe lamp	pH=5, $C_{catalyst}$:C_0 = 5:1, C_0= 20 mg/L	None	300 min	98.7	32
$ZnFe_2O_4$/g-C_3N_4	8 W LED light	C_0=10 mg/L, pH=5, V=40 mL, m=2 mg	CH_3OH	24 h	94.62	34
TT-Por COF-Ni	40 W LED light	C_0=50 mg/L, pH=7, V=10 mL, m=10 mg	None	7 h	97.1	38
PyCMP-3N	300 W Xe lamp	C_0=100 mg/L, pH=6, V=50 mL, m=20 mg	CH_3OH	240 min	99.5	39
CdS(002)/(102)/Ni	300 W Xe lamp	C_0=50 mg/L, pH=5.5, V=50 mL, m=10 mg	None	90 min	97.6	43
$Mn_{0.3}Cdn_{0.7}S$@$Ti_3C_2T_x$	300 W Xe lamp	C_0=100 mg/L, pH=5, V=50 mL, m=10 mg	None	30 min	100	This work

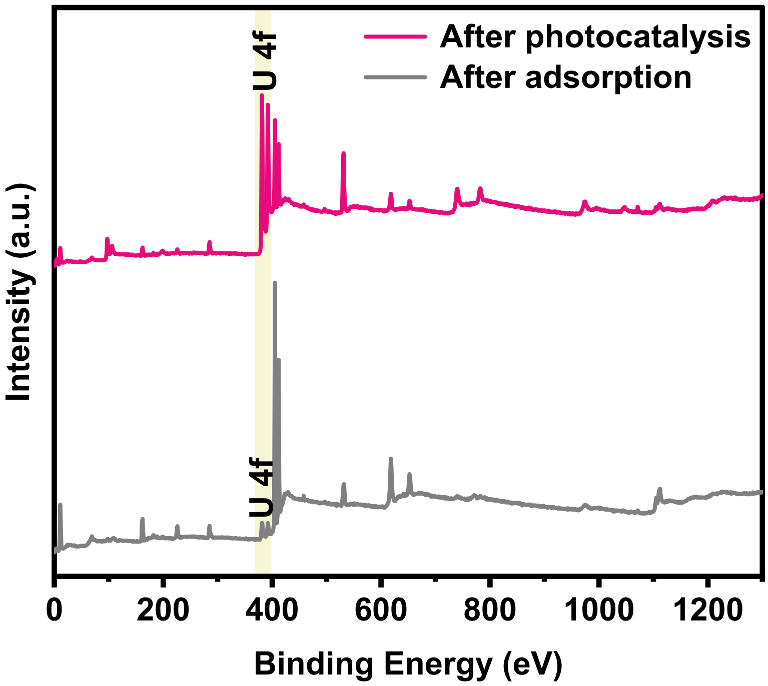

Fig. S3 XPS survey spectra of MCS@TC-15 after adsorption and photocatalysis.

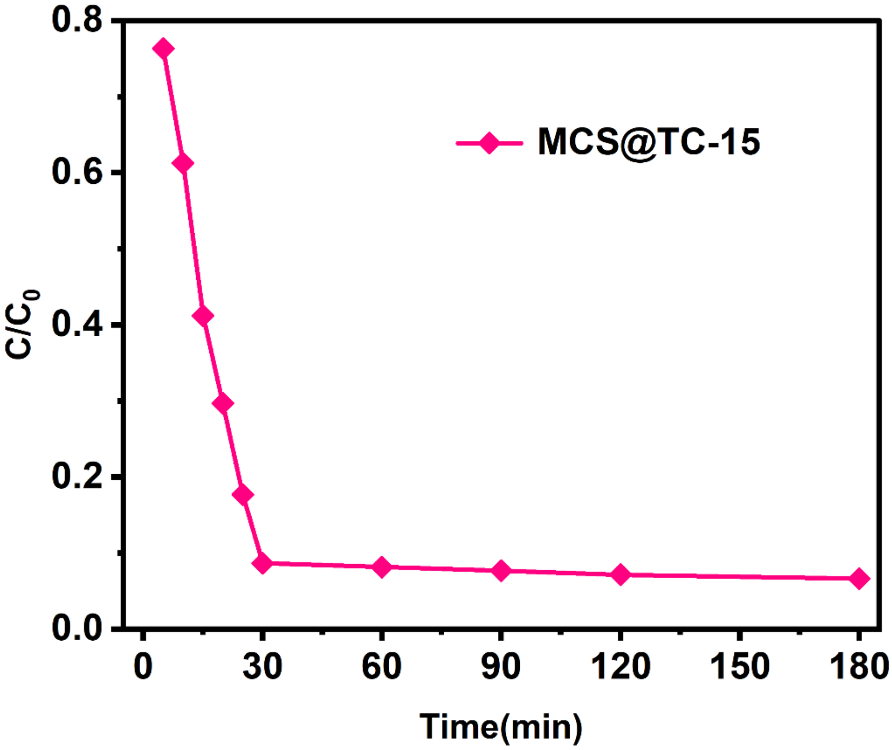

Fig. S4 Time-dependent dark adsorption capacity of MCS@TC-15 for U(VI) (C_0=100 ppm, pH=5, m=10 mg, V=50 mL).

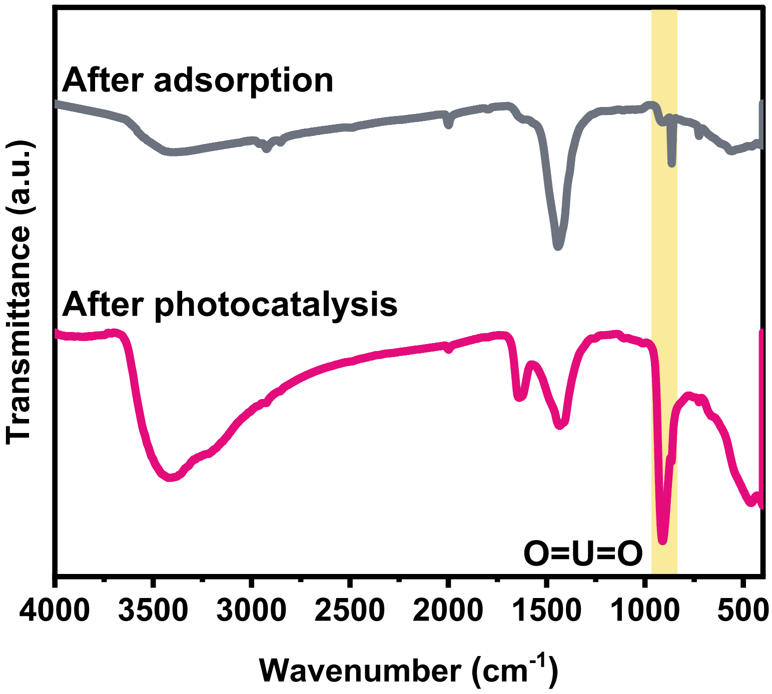

Fig. S5 FT-IR spectra of MCS@TC-15 after adsorption and photocatalysis.

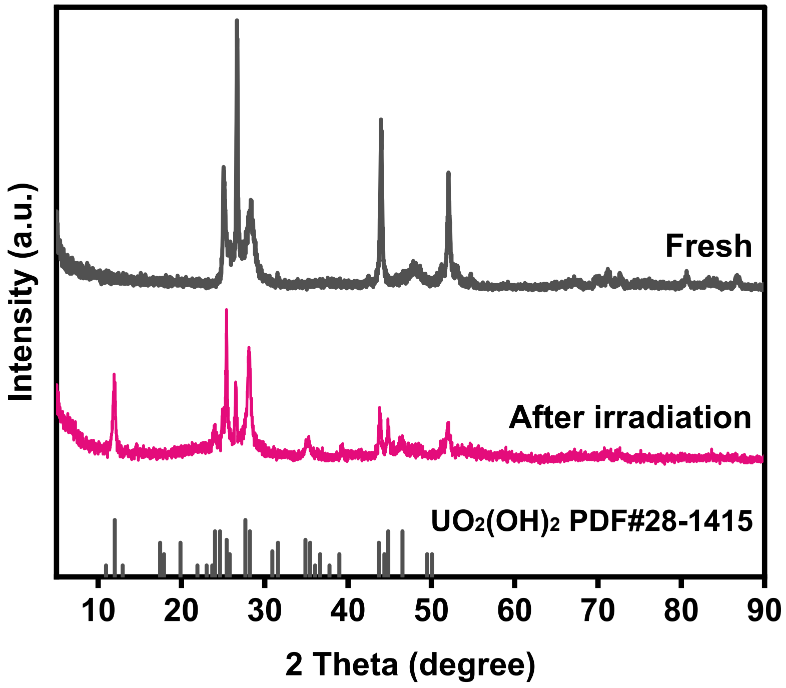

Fig. S6 XRD spectra of MCS@TC-15 before and after photocatalysis.

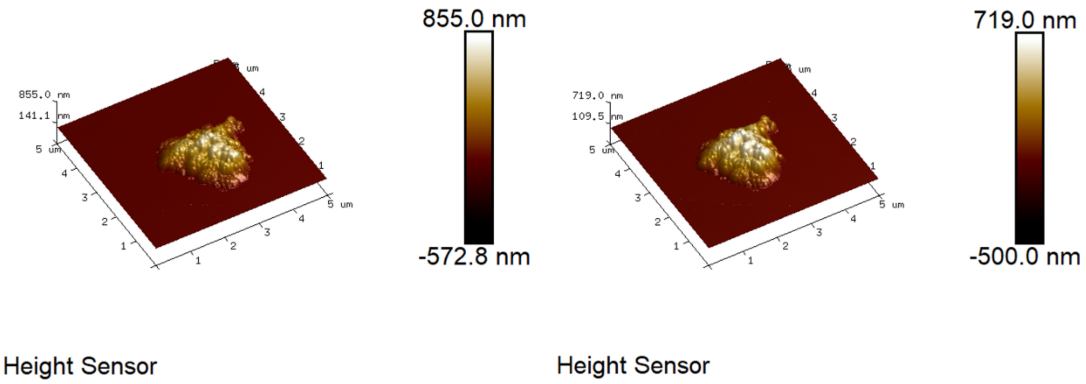

Fig. S7 3D AFM images of MCS@TC-15.

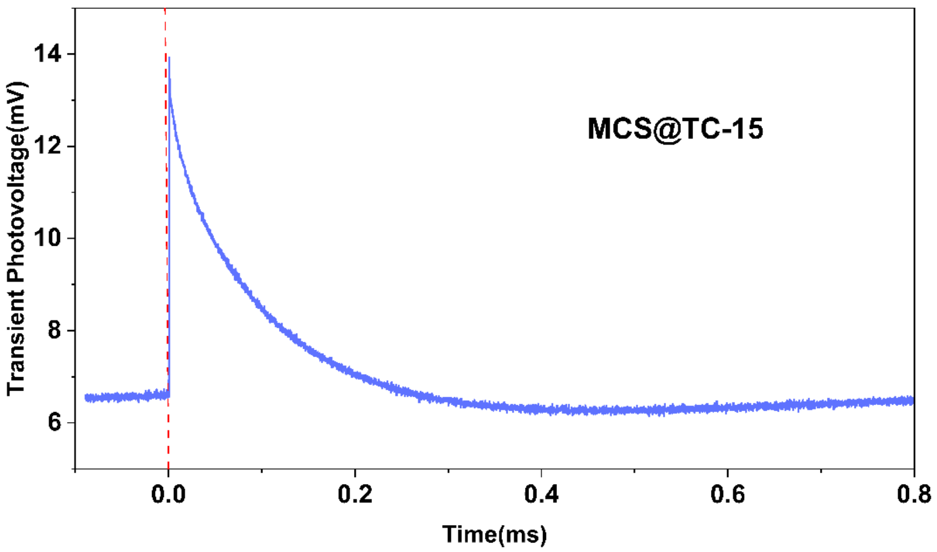

Fig. S8 Transient photovoltage (TPV) spectra of MCS@TC-15 under visible light irradiation.

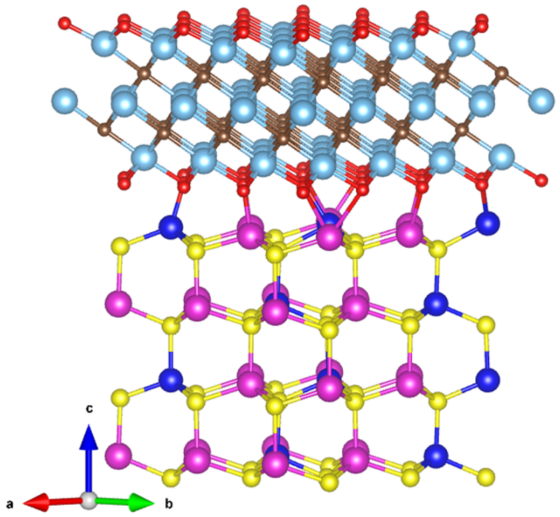

Fig. S9 Structural modelling of MCS@TC-15 heterojunctions.

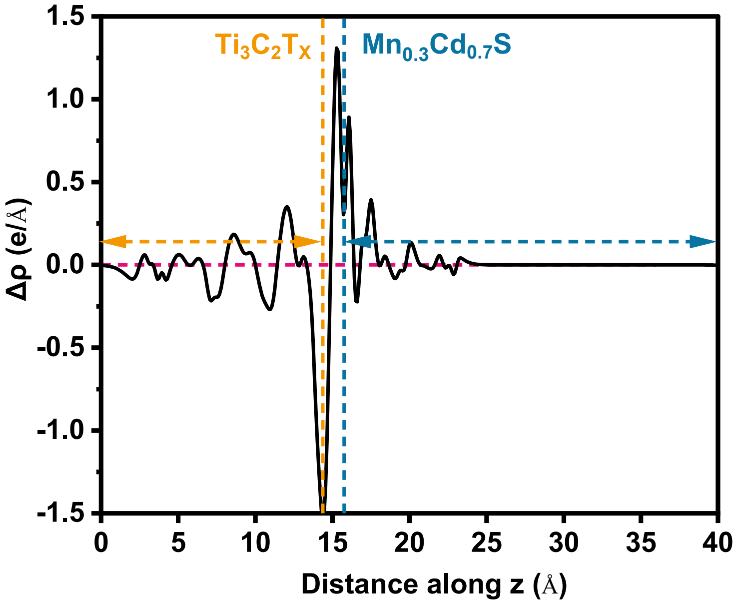

Fig. S10 Planar-averaged charge density difference of $Mn_{0.3}Cd_{0.7}S@Ti_3C_2T_x$ heterojunctions (the dotted lines represent the interface between the two components).